Materials and Design 198 (2021) 109302

Contents lists available at ScienceDirect

Materials and Design

journal homepage: www.elsevier.com/locate/matdes

Experimental and numerical investigation of ply size effects of steel foil reinforced composites

A. Keller [a], R. Geissberger [a], J. Studer [a], F. Leone [a], D. Stefaniak [b], J.A. Pascoe [c], C. Dransfeld [a,c], K. Masania [a,c,*]

[a] Institute of Polymer Engineering, University of Applied Sciences and Arts, Northwestern Switzerland, Klosterzelgstrasse 2, 5210 Windisch, Switzerland
[b] German Aerospace Centre (DLR), Institute for Composite Structures and Adaptive Systems, Lilienthalplatz 7, 38108 Braunschweig, Germany
[c] Faculty of Aerospace Engineering, Delft University of Technology, Kluyverweg 1, 2629 HS Delft, the Netherlands

HIGHLIGHTS

- Thick and thin-ply CFRP laminates were mechanically characterized with and without steel foil reinforcement.
- Local steel foil reinforcement around holes can overcome the notch sensitivity of thin-ply composites.
- The onset (0.5%) and 2% bearing strength of the thick-ply CFRP were more than doubled with the addition of steel foils.
- Onset bearing strength of the hybrid CFRP are also higher than the ultimate strength of the pure CFRP.
- Ply thicknesses may be tuned to generate stable damage propagation in the hybrid configuration.

GRAPHICAL ABSTRACT

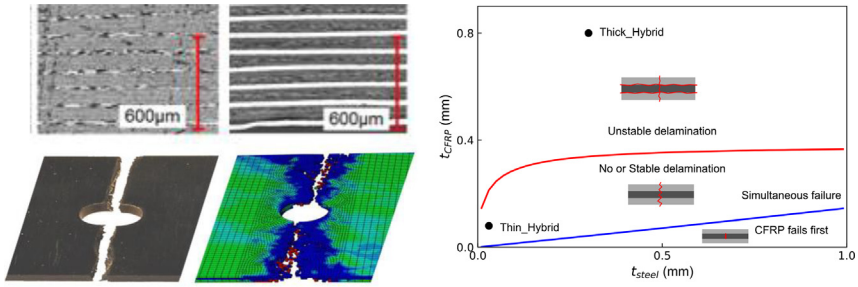

ARTICLE INFO

Article history:
Received 11 October 2020
Received in revised form 4 November 2020
Accepted 5 November 2020
Available online 07 November 2020

Keywords:
Fibre metal laminates
Thin ply composites
Open hole damage

ABSTRACT

The effect of ply thickness on the notch sensitivity and bearing properties on carbon fibre reinforced polymer composites and their hybrid laminates with steel foils were studied. Laminates with ply thicknesses of 0.3 mm and 0.03 mm comprising of CFRP and hybrid laminates were manufactured and characterized using tension, open hole tension and double lap bearing tests. A 25% ply substitution was found to double the bearing load with extensive plastic deformation in the joint while maintaining high stress and maintaining constant cross-sectional thickness in the laminate. With a good agreement between the finite element predicted values and failure behaviour, the damage initiation and progression behaviour could be observed experimentally. We numerically captured (i) rapid failure of 0° plies in the thin ply CFRP hybrid and (ii) continuous delamination with significant plastic deformation for the thick ply CFRP hybrid. The numerical results significantly reduce future experimental work when designing hybrid laminates and could allow the laminate lay-up to be tailored for load cases. Both the experiments and numerical models underline the distinct size effects occurring with respect to the ply thicknesses when hybridising a very ductile metal with a brittle yet strong composite material.

1. Introduction

Aerospace structures are typically composed of carbon fibre-reinforced thermosetting polymers (CFRP) to reduce weight and hence reduce emissions during operation [1]. The high anisotropy of CFRP

* Corresponding author at: Institute of Polymer Engineering, University of Applied Sciences and Arts, Northwestern Switzerland, Klosterzelgstrasse 2, 5210 Windisch, Switzerland.
E-mail address: k.masania@tudelft.nl (K. Masania).

https://doi.org/10.1016/j.matdes.2020.109302

require diverse and complex layups, which are designed depending on the load case of the structure and usually exhibit a multi-directional fibre directions. To achieve these orientations in a cost effective manner, automated manufacturing methods such as tape laying, pultrusion or resin transfer moulding (RTM) are used to build the laminates and to create sub-components that are then joined together [2]. However, the relatively low bearing strength of CFRPs means that the laminate has to be thickened in order to have sufficient joint strength. An option to overcome thick laminates is to only locally increase the thickness of the structure, rather than sizing the entire laminate. Studer et al. showed that co-curing of doublers allow for an increase in the local bearing strength without the addition of substantial weight to the structure [3]. The drawback of this method is the increased load path eccentricity, which requires longer bolts and larger metallic fittings and introduces secondary bending. To avoid local thickening, hybridisation of the composites with metals, into fibre metal laminates (FMLs), can be an attractive solution. The metal layer lead to increased strength in the regions that require higher load carrying capacity, without a resulting change in cross-section. Carbon fibre composites have been hybridised by titanium foil interleaving or substitution in the joint area, with the latter bypassing the need for local thickening of the composite material [4,5]. Steel foils have become an attractive alternative because half of the metal volume is needed compared to titanium foils in order to achieve the same bearing strength at lower material cost. More recently, steel foil hybridisation has shown to improve the bearing strength of CFRP parts [6–9].

The development of thin ply technology has increased ply design freedom, while offering materials with higher sustained stresses until first ply failure. This size effect known as thin ply effect allows for delayed matrix damage, delamination and first ply failure [10]. However, thin ply composites fail in a very brittle manner with little or no warning and have shown high notch sensitivity [11–14]. The notch sensitivity is attributed to the damage suppression and crack-propagation resistance [15]. Using acoustic emission Huang et al. [12] also observed that delamination and matrix cracking during open hole tensile tests were indeed supressed in thin ply laminates.

Steel alloys could therefore be especially suitable as reinforcement in thin ply materials due to their low cost and their high stiffness, strength and elongation at break [16]. Kötter et al. [17] showed that hybridisation of steel foil patches and thin-ply CFRP can improve the open hole tensile and compression strength up to about 30%, especially if applied locally [18–20]. Further work from Bosbach et al. [16] has shown that the addition of metal layers can help to better detect defects when using structural health monitoring to detect delamination.

These works show that the local placement of thin steel foils in critical areas within the load path can reduce the notch sensitivity. The effectiveness of the reinforcement depends on factors such as ply thickness, steel alloy ductility, layup, and design of the transition area. In order to create an optimal laminate design, more understanding of the effect of these factors is needed. In addition, the ability to accurately predict the open hole tension strength for a given laminate design could be of great value.

The aim of this study is to generate the necessary understanding to be able to design hybrid steel foil-CFRP laminates for open hole load cases. The effect of hybridisation of CFRP laminates with ductile steel foils was both experimentally and numerically studied for two different ply thicknesses. Ready to use finite element (FE) models were developed, which can be used to understand the effect of the steel foils, and to design the ply-thickness and number of steel foils for optimal laminate performance. A simple analytical model was also developed to understand to what extent the ductility of the steel layers can be used to improve the hybrid laminate's failure strain and energy absorption capability.

2. Materials

The CFRP material used in this study [21] was a Toray M40JB Prepreg, CFRP ThinPreg TM 80EP-736/CF, from North Thin Ply Technology SARL, Switzerland, Two different ply areal weights were used, namely 30 g/m^2 (Thin) and 300 g/m^2 (Thick). The prepregs were processed into quasi-isotropic composites by a sequence of ply stacking into subunits of 4, debulking for 30 min at 4 mbar and repeating until the laminate stack was completed. The laminates were cured using a hot press at 80 °C and 0.6 MPa (6 bar) pressure for 8 h using a "LaboPress P200T", Vogt, Germany. For the hybrid CFRP plates, austenitic CrNi-stainless steel 1.4310 at the equivalent thickness of the 90° ply in the substituted laminate (0.03 mm or 0.3 mm) was first prepared. A process very similar to the Boeing sol-gel surface treatment was adopted [22] to improve the steel foil to CFRP adhesion. Following this process, the steel surface was degreased and then deoxidized by using a continuous vacuum blasting method. Finally, an aqueous sol-gel system, a dilute solution of a stabilized alkoxy zirconium organometallic salt and an organosilane coupling agent, was applied. The 90°-layers of the carbon fibre composite were substituted with steel foils, as described in Table 1 and shown also in the polished optical cross sections in Fig. 1.

3. Methods

3.1. Experimental

Samples for optical microscopy were prepared by embedding the samples in epoxy and preparing them in a "TegraPol-21", polishing machine from Struers GmbH, Switzerland. The samples were polished using a diamond polishing solution with a minimum particle size of 0.25 μm in the paste. Images of the optical cross-sections were taken using a "VKX-200", Keyence, Germany, 3D laser scanning microscope.

Open hole tension tests were performed in accordance to ASTM D5766M-95 with an H6 6 mm hole. Unnotched tensile tests were also performed, in accordance to ISO 527-00. A constant displacement rate of 1 mm/min was used for all samples, recording force and both machine and extensometer displacement.

Double lap bearing tests were performed following ASTM D5961M-08, with 8 mm bearing fasteners (f9/H6 fit, class 12.9 high strength steel). Again, a constant displacement rate of 1 mm/min was used for all samples and the machine and extensometer displacement were recorded.

A universal testing machine from Walter and Bai, Switzerland, with a 100 kN capacity load cell of was used for all mechanical tests. The specimen gauge lengths were 24 mm for the open hole tensile and unnotched tensile tests, and 50 mm for the double lap bearing tests.

3.2. Numerical

Abaqus 6.1 (Dassault Sysèmes) was used to model a 3D explicit damage model of both the CFRP and hybrid composites. The model was separated in distinct regions, which were individually formulated, as shown in Fig. 2(a). C3D8R hexagonal elements were used in a quarter geometry continuum model with an orthotropic material. A 3D damage VUSDFLD sub-routine with a Hashin 3D failure criterion [23] was used with a layered structure (shown in red in Fig. 2(a)). The steel foils were modelled as elastic-plastic material using a Johnson Cook [24] formulation for the 1.4310 austenitic stainless steel combined with experimental data.

Table 1
Material designation and lay-up of the carbon fibre and hybrid laminates.

Sample	Layup	Ply thickness (mm)	Density (kg/dm^3)
Thin_CFRP	[90°,45°,0°,-45°]10$_s$	0.03	1.6
Thick_CFRP	[90°,45°,0°,-45°]$_s$	0.3	1.6
Thin_Hybrid	[St,45°,0°,-45°]10$_s$	0.03	3.18
Thick_Hybrid	[St,45°,0°,-45°]$_s$	0.3	3.18

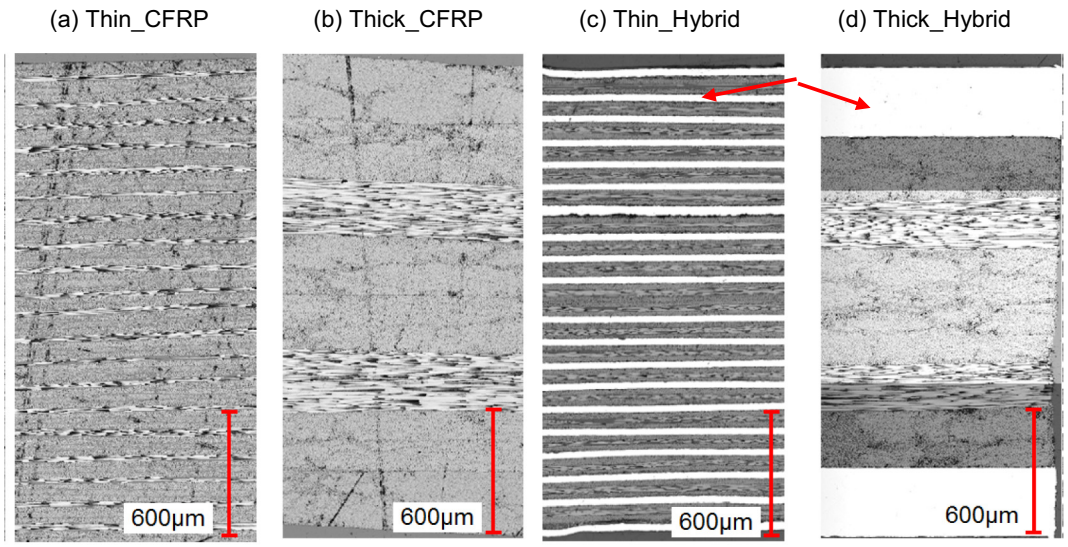

Fig. 1. Polished optical sections of the carbon fibre and hybrid laminates. Steel foils are appear as white layers and are indicated by red arrows. (For interpretation of the references to colour in this figure legend, the reader is referred to the web version of this article.)

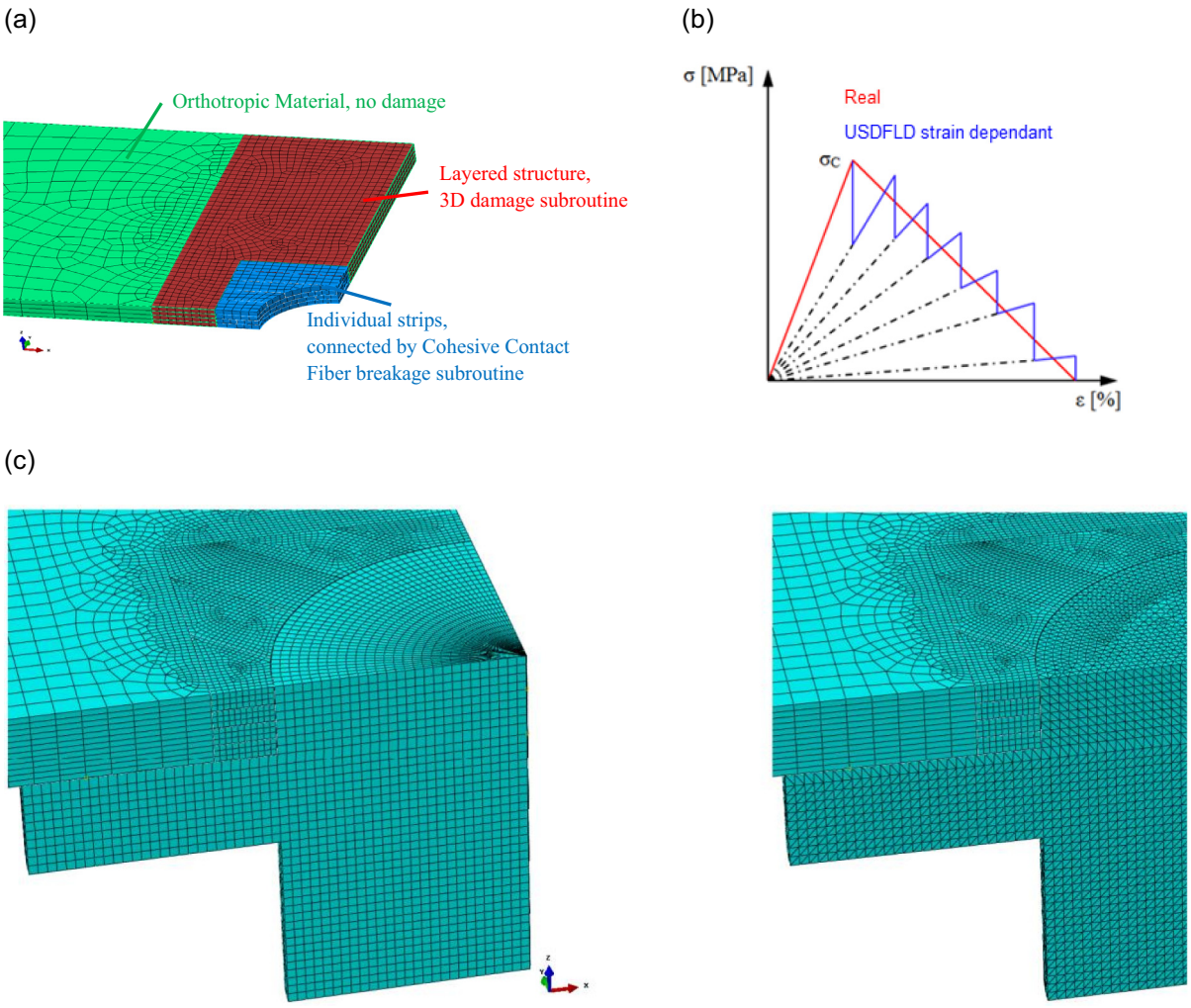

Fig. 2. (a) Schematic of the developed quarter model with regions of varying complexity for the open hole tensile simulations, (b) element strain dependant degradation and (c) the quarter model for the bearing test simulations.

The element stiffness can be reduced using field variables. While they are relatively easy to implement, they lack the ability to replicate the actual failure process. Therefore, to better model the stress-dependent elongation shown in Fig. 2(b), a strain dependant progressive stiffness decrease was implemented. To do this, the stress was calculated at each time step, the failure was checked using the 3D Hashin criterion and the element stiffness was reduced accordingly.

The contact between the bolt and the laminates were modelled using a penalty friction coefficient of 0.2 [25] in tangential direction. A hard contact boundary condition was assigned in the normal direction. To account for the ability of fibres which fail in compression to still partially contribute to the laminate stiffness, the stiffness of the failed areas was set to 30% of their original stiffness [26].

4. Results

4.1. Tensile and open hole tensile tests

The stiffness of the notched samples was significantly higher for the hybrid materials, due to the addition of the stiff steel layers (Table 2).

The ultimate tensile strength for unnotched Thin_CFRP and Thick_CFRP was measured to be 750 ± 11 MPa and 554 ± 19 MPa, respectively, resulting in an increased strength of about 30% for the thin-ply laminates (Table 3). Steel foil hybridisation further increased the tensile strength to 994 MPa for the Thin_Hybrid and 942 MPa for the Thick_Hybrid, showing a significant improvement in comparison to the Thick_CFRP of 70%.

Despite the higher unnotched tensile strength, the Thin_CFRP showed a significantly lower open hole tensile strength and hence higher notch sensitivity, with a value of 328 MPa, 28% lower than the Thick_CFRP with 453 MPa. Different failure behaviours were observed for the CFRP composites, as shown in Fig. 3. In the Thin_CFRP samples, a near horizontal tensile crack was observed through the sample with dominant fibre fracture and little delamination present. The samples with conventional laminate ply thickness, however, showed delamination prior to failure around the hole. Failure was also observed in the 45° layers. As expected in the Thin_CFRP samples, the very thin plies supress delamination, which reduces fibre pull-out and load redistribution during damage, leading to premature and brittle failure, as was also noted by Amacher et al. [10]. It can be seen in the stress-strain curves in Fig. 4 that the stress in the Thin_CFRP increased linearly until failure, whereas in the Thick_CFRP a reduction in stiffness was observed before the ultimate stress. The stress peaks around the hole were reduced through matrix failure in the Thick_CFRP. The reduced notch sensitivity of the Thick_CFRP is related to the strong delamination, as during delamination the ±45° fibre plies align in the direction of load, which was also noticed in the hybrid laminates.

Hybridisation of the CFRP showed far greater contribution to improvement of open hole strength for the Thin_Hybrid, which demonstrates that hybridisation helps to decrease the high notch sensitivity of thin-ply composites. While again, the open hole tensile strength of the Thick_Hybrid was higher with 589 MPa in comparison to 535 MPa for the Thin_Hybrid, the difference is less than for the pure CFRP samples. The Thin_Hybrid failed catastrophically without plastic deformation of the whole laminate, as can also be seen in the stress-strain curves in Fig. 4. Only a small non-linearity was observed for the Thick_Hybrid. Necking of the steel plies was observed in the Thick_Hybrid specimens but not in the Thin_Hybrid specimens, adding additional evidence that there was more plastic deformation in the Thick_Hybrid case.

The typical failures of the hybrid materials are similar to those of the CFRP samples and can be seen in Fig. 3. Even though the specific strength of the hybridised materials is lower compared to the CFRP samples, the strength gains and the pseudo-ductile failure behaviour could justify the use of steel foil localised around a hole, avoiding a significant weight penalty by allowing a reduced thickness in the rest of the part, as will be discussed further in the Discussion section.

Table 2
Open hole tensile stiffness of the carbon fibre and hybrid laminates.

Sample	OHT stiffness (GPa)	Specific OHT strength (GPa dm^3/kg)
Thin_CFRP	58 ± 2	36
Thick_CFRP	66 ± 12	41
Thin_Hybrid	97 ± 9	30
Thick_Hybrid	102 ± 6	32

Table 3
Tensile and open hole tensile strength of the carbon fibre and hybrid laminates.

Sample	Tensile strength (MPa)	OHT strength (MPa)	Specific OHT strength (MPa dm^3 / kg)	Notch sensitivity
Thin_CFRP	750 ± 11	328 ± 7	205	2.29
Thick_CFRP	554 ± 19	453 ± 49	283	1.22
Thin_Hybrid	994	535 ± 6	168	1.86
Thick_Hybrid	942	589 ± 40	185	1.60

4.2. Double lap bearing tests

The double lap bearing onset (0.5% strain offset) strength of the Thin_CFRP and Thick_CFRP were measured to 457 MPa and 356 MPa, respectively, resulting in a 28% higher strength of the Thin_CFRP (Fig. 5). The suppression of transverse cracking and delamination in the Thin_CFRP that was observed in the tensile tests has similarly improved the bearing performance of the composite material.

Increased bearing strength was measured for both hybrid laminates. The onset strength for the Thick_Hybrid (803 ± 76 MPa) was more than double the Thick_CFRP composite value (356 ± 46 MPa).The specific onset strength for the Thick-Hybrid specimens was also higher, relative to the Thick-CFRP specimens (Table 4). The measured onset strength of the Thick_Hybrid (803 ± 76 MPa) was even higher than the ultimate strength of both the Thick_CFRP (562 ± 17 MPa) and the Thin_CFRP (720 ± 17 MPa).

After testing the CFRP samples were embedded and sectioned and shown in Fig. 6(a) and (b). The Thin_CFRP samples showed only very localised damage on the surface, as shown in Fig. 6(a). A 22 mm wide delamination area was observed in the 90° layer, next to some kinking of plies leading to fibre failure under compression, whereas in the Thick_CFRP a much larger delamination of about 40 mm wide in the 90° layer and fibre breakage was observed in Fig. 6(b). Therefore, compressive, shear failure appears to be the main failure mechanism in Thin_CFRP. In contrast, the Thick_CFRP appears to fail in delamination related modes, which lead to buckling and compression.

The hybrid laminates showed buckling and failure in shear and compression, as shown in Fig. 6(c) and (d). Furthermore, brooming was observed on the compressive side of the hole, due to bolt indention.

Shear kink bands projected along the washer supported area and appeared in the washer confined area of the laminate. The Thin_Hybrid lacked transverse ply breakage, indicating suppression of delamination. In contrast, a significant amount of composite material between the steel foils fell out for the Thick_Hybrid microscopy samples during preparation, indicating extensive delamination and damage that occurred during the test.

The adhesion between the CFRP and steel foils seems to be relatively strong, as shown in the higher resolution images in Fig. 6(c) and (d). No adhesive failure is visible despite the large deformation. However, no adhesion measurements have been conducted yet.

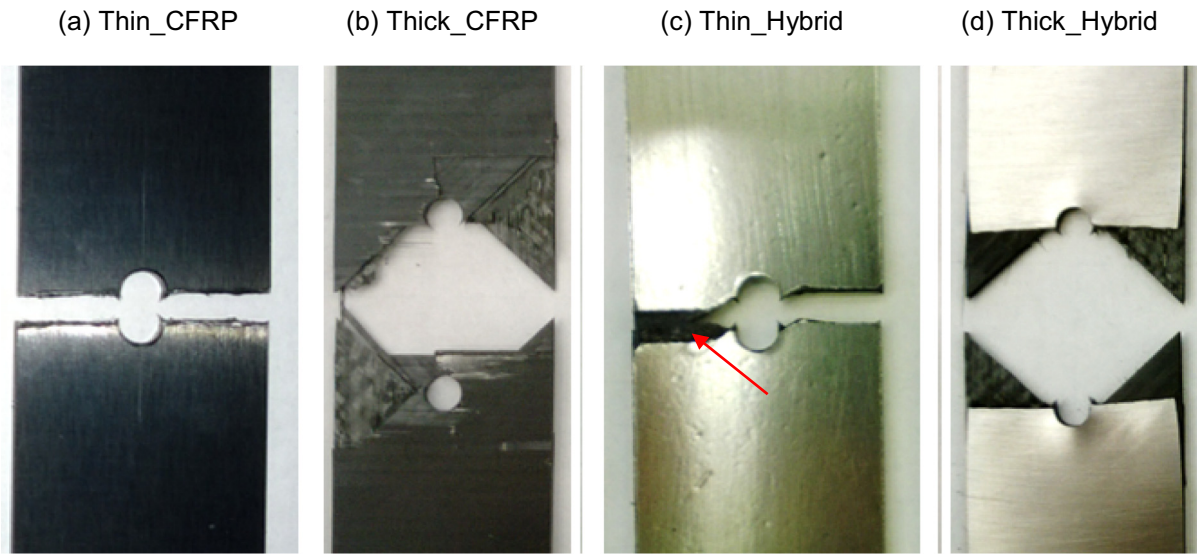

Fig. 3. Images show the open hole tensile failure of the carbon fibre and hybrid laminates. It can be seen that metal ductility is supressed in the thin-ply hybrid (red arrow), while necking occurs in the thick ply hybrid. (For interpretation of the references to colour in this figure legend, the reader is referred to the web version of this article.)

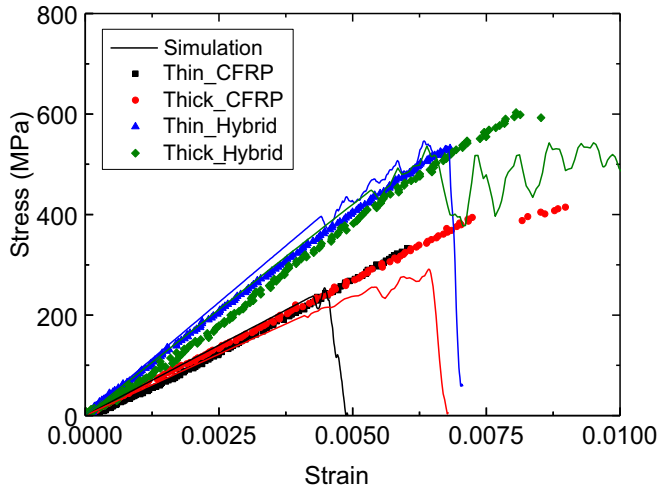

Fig. 4. Comparison of open hole tensile stress-strain curves between experiments (dots) and simulations (lines) for the carbon fibre and hybrid laminates.

4.3. Numerical modelling results

A comparison of open hole tensile tests and simulations is shown in Fig. 8, with an agreement of the stiffness between numerical and experimental results. The numerical model slightly underpredicted the failure stress of the Thin_CFRP and Thick_CFRP. However, the delamination progression shows better agreement. The Thin_CFRP model shows matrix damage only very close to the crack and no delamination was observed around the hole, as seen from the matrix tensile failure results in Fig. 7. In contrast, the Thick_CFRP model has matrix damage in a large area around the crack and several elements are detached, indicating delamination failure. Those results are in excellent agreement with the experimentally observed failure of the composites shown in Fig. 4.

A good correlation between numerical results and experiments was also achieved for the steel foil hybrid laminates. The Thin_Hybrid showed prompt failure (modelled with element deletion) of the 0° plies, resulting in steel ply failure. A steadier delamination was predicted for the Thick_Hybrid with plastic failure after delamination, as was also experimentally observed.

A comparison between numerical and experimental results for the double lap bearing case is shown in Fig. 8. The models were only run until net tension failure was calculated, which explains why they end far sooner than the mechanical tests. The models show agreement for the maximum stress. Only the Thin_CFRP shows some deviation where the model underpredicted the maximum stress by about 21%.

The numerically calculated area of fibre damage was slightly larger for the Thin_Hybrid than for the Thick_Hybrid, as shown in Fig. 9. This is believed to be because of stronger matrix failure and delamination in the Thick_CFRP, which resulted in slightly less load being transferred to the fibres.

5. Discussion

The experimental results showed several interesting features for each sample. While the unnotched tensile strength can be increased by using thin plies (Thin_CFRP), the open hole tension strength dropped by 28% in comparison to the Thick_CFRP. The stress peaks around the

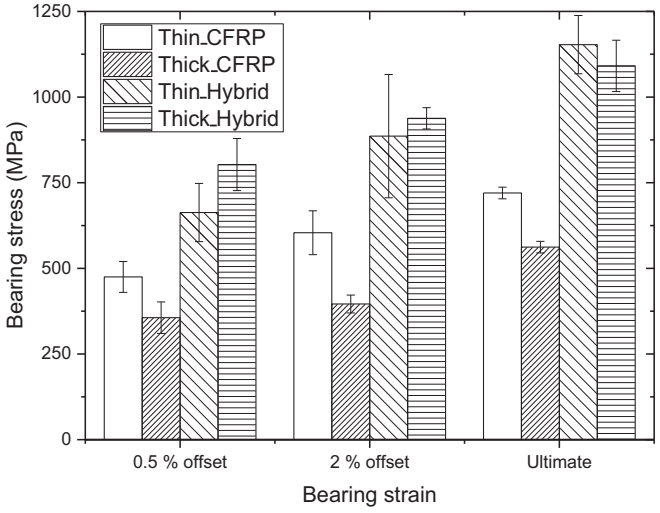

Fig. 5. Comparison of the double lap bearing strength for the carbon fibre and hybrid laminates with progressively increasing bearing strain offsets.

Table 4
Double lap bearing strength of the carbon fibre and hybrid laminates.

Sample	Thin_CFRP		Thick_CFRP		Thin_Hybrid		Thick_Hybrid	
Bearing stress	Mean (MPa)	Specific (MPa.dm^3/kg)	Mean (MPa)	Specific (MPa.dm^3/kg)	Mean (MPa)	Specific (MPa.dm^3/kg)	Mean (MPa)	Specific (MPa.dm^3/kg)
0.5% Offset	457 ± 45	286 ± 28	356 ± 46	223 ± 28	663 ± 85	209 ± 27	803 ± 76	253 ± 24
2% Offset	604 ± 64	247 ± 16	396 ± 26	248 ± 16	886 ± 180	279 ± 56	938 ± 31	295 ± 10
Ultimate	720 ± 17	450 ± 10	562 ± 17	351 ± 11	1153 ± 85	362 ± 27	1091 ± 75	343 ± 24

hole can be reduced through matrix failure in the Thick_CFRP, which is not possible when using Thin_CFRP. In contrast, the bearing failure is more dominated by interlaminar properties, and hence the Thin_CFRP showed about 28% higher bearing strength.

The hybrid laminates show similar maximum stresses irrespective of ply thickness, resulting from the stress transfer to the steel foils. Delamination of the steel foils was not observed for open hole tensile tests for the Thin_Hybrid, leading to a brittle and catastrophic failure. In contrast, the damage behaviour of the Thick_Hybrid specimens were found to be a combination of premature metal foil delamination and subsequent fibre failure. Interestingly, stress concentrations around raptured fibre ends could be accommodated by the ductile metal foils.

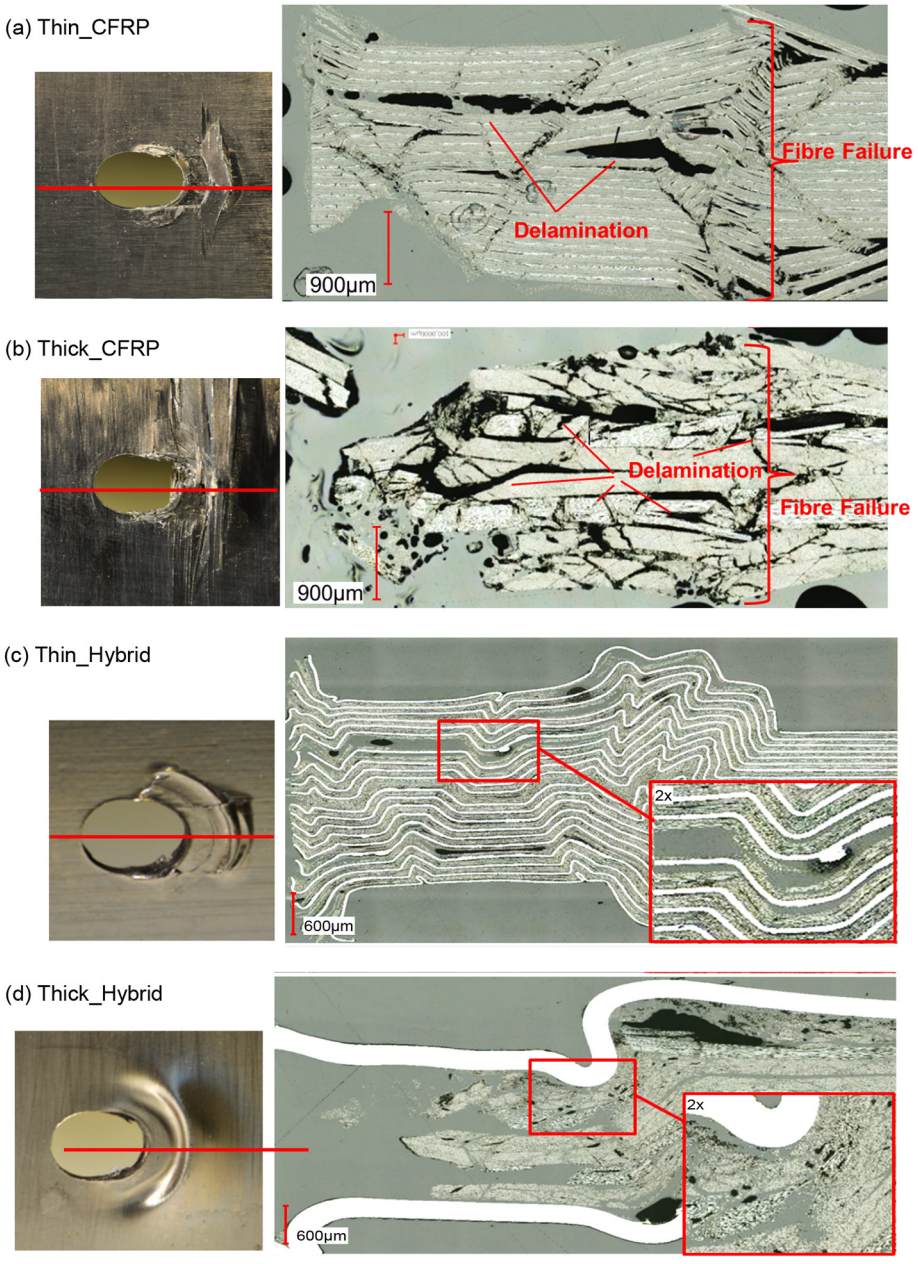

Fig. 6. Comparison of the bearing failure (a-d). The left of the image indicates the bolt location (compression side) and the right of the image shows the damaged portion of the composite material from sample cross-sections.

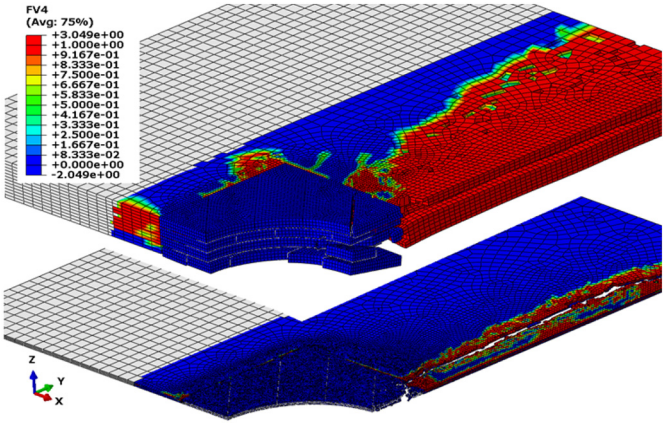

Fig. 7. Above, Thick_CFRP and below Thin_CFRP laminate simulation results indicating matrix tensile failure resulting in delamination in OHT.

The specific strength of the open hole tensile tests and the double lap bearing tests were found to be lower with the addition of steel foils. However, the steel foils can be localised around a hole in order to design a thinner structure with the necessary strength, which can actually reduce the total weight of the connection due to shortened clamping area and bolt length, and hence reducing load eccentricity. To give a specific example, in a case where the laminate is sized for open hole tension, the Thin_Hybrid OHT strength is 20% higher than that of the Thick_CFRP laminate. Therefore, a Thin_Hybrid laminate can be made 20% thinner for the same strength. The steel reinforcement is only required around the hole, and can be omitted elsewhere. Based on the ratio of densities (see Table 1), if the area where no reinforcement is needed is 4.9 times larger than the area around the holes where the steel is applied, this design will be weight neutral. If the unreinforced area is more than 4.9 times the area of the reinforcement, then the thinner, locally reinforced, laminate will be lighter than a thicker, pure CFRP panel, for the same OHT strength.

Generally, a good agreement between the FE models and the experimental behaviour was found in this study. The values of the bearing strength and the failure behaviour was predicted relatively well. Also, the stiffness of the OHT tests showed good agreement. Some deviation was found for the Thin_CFRP strength and strain. These models might therefore be used to predict mechanical strength of different layups, and hence can be used to optimise the lay-up according to the load case during structural design.

Effect of foil thickness on ductility

The Thick_Hybrid and Thick_CFRP specimens exhibited a higher failure strain than respectively the Thin_Hybrid and Thin_CFPR specimens, indicating an increased energy absorption capability for the Thick laminates. This is likely due to the ability of the Thick laminates to delaminate and pull-out the $\pm 45°$ plies, as can also be seen in Figs. 3 and 4. Additionally, Fig. 3 points to the importance of plastic deformation in the steel layers. In the Thin_Hybrid specimens, plastic deformation in the steel seems to be very limited, whereas the Thick_Hybrid specimens show signs of necking, indicating that plastic deformation occurred over a larger area.

To maximize the laminate failure strain and energy absorption, as much of the steel as possible should be free to reach its own failure strain, which is much higher than that of the CFRP layers, i.e. > 10% and 1%, respectively. However, in all the regions where the steel is perfectly bonded to the CFRP layers, it will not be able to strain more than the failure strain of the CFRP. This means that delamination between the CFRP and steel layers is actually beneficial during open hole tension, as it will allow more for the steel to plastically deform and reach its individual failure strain. Rehra et al. [27] have also recently shown analytically that more delamination is beneficial in this case.

To enable delamination, the strain energy release rate (SERR) needs to locally exceed the fracture toughness in the interface. If the laminate thickness is kept constant, then the total strain energy release is not dependent on the ply thickness. However, a lower ply thickness means this energy release will be distributed over more interfaces, significantly reducing the SERR in each interface. To promote delamination, it is therefore beneficial to have fewer interfaces and thus thicker plies. Note that any surface treatments applied to the steel, to improve the adhesion of the epoxy, inhibit delamination. This is detrimental to achieving the maximum laminate failure strain.

Having large scale delamination can be beneficial to failure strain, and therefore energy absorption. However, unstable delamination propagation across the entire interface would again reduce the energy absorption capabilities, as noted in Czél and Wisnom's analysis of hybrid composites [28].

The occurrence of unstable delamination propagation can be predicted using the criterion provided by Czél, Jalalvand and Wisnom [29]. Rewriting this in terms of the thickness ratio gives:

$$G_{IIc} > G_{II} = \frac{\varepsilon_{f,CFRP}^2 E_{CFRP} t_{CFRP} \left(2E_{Steel} + E_{CFRP} \frac{t}{t_{Steel}}\right)}{8E_{Steel}} \quad (1)$$

where ε_f is the failure strain, G_{IIc} is the mode II fracture toughness, E is the Young's modulus, t is the thickness, and the subscripts *Steel* and *CFRP* refer to the respective layers. As Eq. (1) was developed for a unidirectional layup, equivalent values for each CFRP sublaminate block should be used for E_{CFRP} and t_{CFRP}. The equation shows that the larger the thickness ratio, the higher the SERR. Due to the need of having large delaminations between the steel and CFRP layers, optimum performance is achieved when approaching the criterion of Eq. (1), without exceeding it, and the ply thickness ratios should be tuned accordingly.

To maximize ductility of the laminate, the steel layers should remain intact and deform further after the first failure in the CFRP plies occurred. In the ideal case, one could then obtain a laminate failure strain equal to the steel failure strain. Assuming that the total force on the laminate before and after failure of the CFRP ply must be equal, one can write:

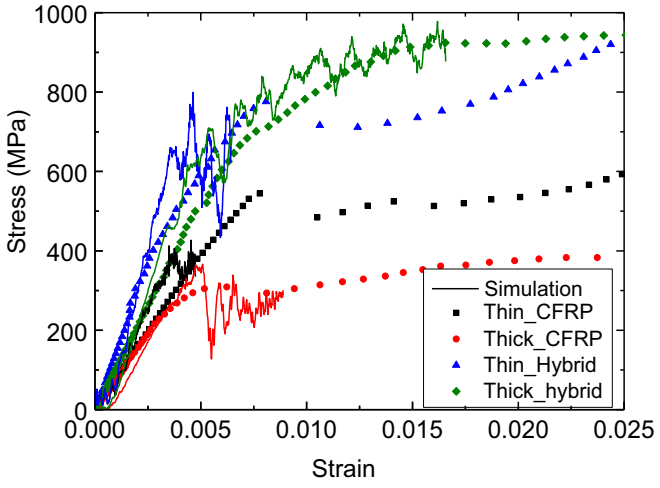

Fig. 8. Comparison of double lap bearing stress-strain curves between the mean of experiments (dots) and simulations (lines).

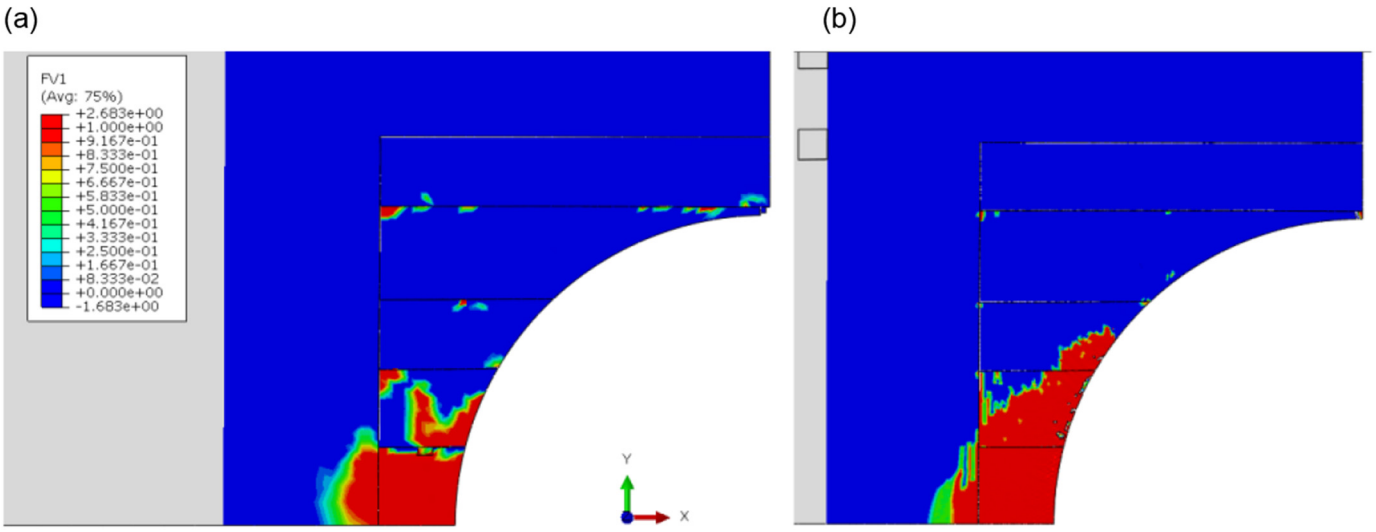

Fig. 9. Fibre compression failure indicated in red for (a) the Thick_hybrid and (b) the Thin_Hybrid laminates during bearing strength simulation. (For interpretation of the references to colour in this figure legend, the reader is referred to the web version of this article.)

$$\sigma_{ult,steel} = \sigma^*_{steel} + \sigma^*_{CFRP}\frac{t_{CFRP}}{t_{steel}} \tag{2}$$

where σ* refers to the stress in the layer at the moment the CFRP fails.

Using Eqs. (1) and (2), with material data from the Metallic Materials Properties Development and Standardization (MMPDS) document [30] for the steel, and from Amacher et al. [10] for the CFRP, the failure map shown in Fig. 10 can be drawn. This map shows the expected failure mode as a function of steel and CFRP ply block thicknesses. The map indicates that a very high steel to CFRP ratio would be needed to prevent failure of the steel as soon as the first CFRP failure occurs. The calculation of the ultimate stress criterion took into account the effect of ply thickness on the tensile strength of an isotropic laminate, as reported by Amacher et al. [10]. However, for the steel it was difficult to find good data on the stress-strain behaviour at higher strain levels. Therefore σ^*_{steel} was set equal to the stress at a strain of 1%, based on the data from the MMPDS [30]. This possibly underestimates the stress in the steel layers at the moment of ply failure. If the stress in the steel layers increases, the slope of the 'ultimate stress criterion' line in the failure map will reduce, implying that an even higher steel to CFRP ratio would be required to keep the steel layers intact.

The two laminates tested in this work have been indicated in the map, using the post-cure thicknesses measured from Fig. 1. It can be seen that the Thin_Hybrid laminate exceeds the strength criterion, but is below the fracture toughness criterion, which predicts that the steel plies would fail almost immediately after the first failure in the CFRP ply, with little pull-out or plastic deformation in the steel plies. This matches what was observed in the experiments (Fig. 3(c)). The Thick_Hybrid laminate exceeds both the strength and the fracture toughness criteria. This suggests that the steel layers would fail immediately upon failure of the CFRP plies, and that large delaminations could also occur. This matches the failure pattern observed in the images in Fig. 3(d).

Based on Fig. 10 we can hypothesise that maximum laminate ductility can be achieved by choosing a combination of ply thicknesses that would fall below the ultimate stress criterion; bearing in mind that t_{CFRP} in Eqs. (1) and (2) refers to the thickness of the total ply block of CFRP plies between two steel layers, not to the individual ply thickness. This implies that to achieve maximum ductility, one would have to use steel layers that are an order of magnitude thicker than the CFRP plies.

The failure map shown in Fig. 10 does not include the effect of thermal residual stresses. Given the mismatch in the coefficient of thermal expansion between the steel and the CFRP, during post-cure cooling, a tensile stress will be induced in the steel layers, and a matching compressive stress in the CFRP plies. This residual tensile stress means that the steel plies are somewhat closer to failure already, and thus the maximum CFRP thickness for a given steel thickness to avoid the ultimate stress criterion (Eq. (2)) will be reduced. Similarly, thermal residual stresses will induce a shear stress between the steel and CFRP layers. Consequently, for a given loading the SERR is closer to G_{IIc} than would be predicted based on an analysis that neglects the residual stresses. The magnitude of the shear stress will depend on the number of interfaces in the laminate, which, for a given laminate thickness, is a function of the ply thickness. The effect of thermal residual stresses may also be mitigated through cure shrinkage of the CFRP layers. More research is therefore needed to understand the post-cure residual stress state in the laminate, and how this affects the failure modes.

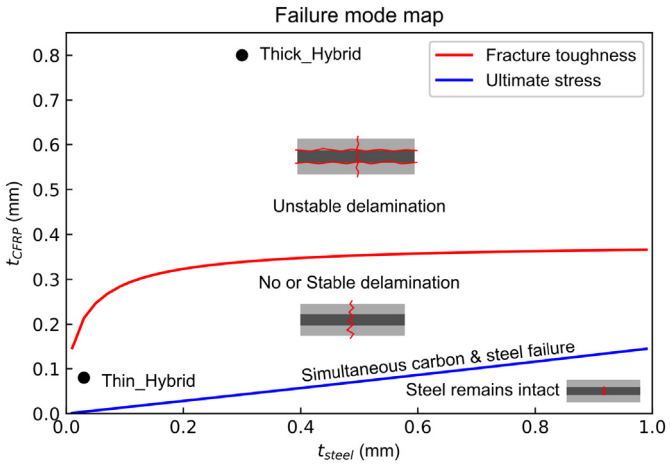

Fig. 10. Failure modes for different combinations of steel and CFRP ply thickness. The two laminates tested during this work are also indicated, using t_{CFRP} values measured from Fig. 1. Note that t_{CFRP} here indicates the thickness of the total block of CFRP plies between two steel layers.

Concluding this section, the analysis suggests that, unless one uses very high steel to CFRP thickness ratios, it is not possible to make optimal use of the steel's ductility, as the steel layers will fail almost immediately when the CFRP layers fail. However, laminate failure strain and energy absorption can be improved by allowing delamination to occur, which implies selecting a combination of thicknesses close to or above the unstable delamination criterion. For example, from Fig. 10 we can hypothesise that in a thin-ply layup with 8 or 12 ply quasi-isotropic blocks between the steel foils, delamination would occur, as the laminate would be above the delamination criterion. This would likely reduce the notch sensitivity of the laminate, allowing more optimal use of the increased strength of the thin-ply material. Apart from adjusting the ply thickness ratio, one can also influence interface strength by changing the surface treatment of the steel layers, which will affect the adhesion between the steel and the epoxy, and therefore the value of G_{IIc}.

6. Conclusions

The open hole tensile and bearing strength of Thin_CFRP and Thick_CFRP were successfully increased by steel foil hybridisation. Hybridisation increased the Thin_CFRP OHT strength by 63%, allowing a significant decrease in thickness to achieve the same strength as without steel foils. Furthermore, the Thin_Hybrid can be almost 20% thinner than the Thick_CFRP to achieve the same OHT strength. The laminate thickness is likely driven by the strength needed around the hole. Therefore, by applying the steel foils locally around the hole an overall thinner laminate can be used.

The smaller the ratio of reinforced to unreinforced area, the larger the weight savings, with a maximum of 20%, corresponding to the reduction in thickness. Hence, a local steel foil substitution with 20% of the total laminate area leads to a lighter and thinner part in comparison to a pure CFRP part with the same strength.

The use of steel foils avoids the need to add more carbon fibre plies in areas to be reinforced, which would require additional debulking cycles, as well as introduce load path eccentricity. This novel approach is especially interesting for thin-ply materials to overcome the high notch sensitivity while keeping the general advantages, i.e. high tensile and compression strength, with the compromise of reduced mass specific mechanical performance. The onset bearing strength for the Thick_Hybrid was even higher than the ultimate strength of both CFRP composites, with similar values for the specific bearing strength.

The developed finite element models can provide good predictions of the OHT strength, as well as identify which failure modes will occur. In future research they can therefore be used to optimise laminate design and to tune the ply thickness and layup to obtain desirable failure behaviour, e.g. to promote delaminations to reduce notch sensitivity. They can also be utilised to optimise the specific strength of the hybrid laminates, and to understand whether there are trade-offs between ultimate strain, notch sensitivity and unnotched tensile strength. These models could also be used to further study the stress distribution in the transition zones between metal and CFRP layers, which can affect delamination initiation. To enable local reinforcement designs on an industrial level, further investigations are necessary to understand what radius around a hole needs to be reinforced in order to obtain the increased open hole and bearing strengths.

CRediT authorship contribution statement

A. Keller: Investigation, Writing - review & editing. **R. Geissberger:** Investigation, Formal analysis. **J. Studer:** Methodology. **F. Leone:** Investigation. **D. Stefaniak:** Resources, Methodology. **J.A. Pascoe:** Visualization, Writing - review & editing. **C. Dransfeld:** Supervision, Writing - review & editing, Funding acquisition. **K. Masania:** Conceptualization, Supervision, Writing - original draft, Writing - review & editing.

Declaration of Competing Interest

The authors declare no competing interests.

Acknowledgments

This work was carried out within the collaborative research project Cost Effective Reinforcement of Fasteners in Aerospace Composites (CERFAC) funded by the European Commission, grant agreement no. 266026, within the Seventh Framework Programme. The authors thank C. Gosrani and W. Woigk for helpful comments and feedback.

References

[1] C. Soutis, Fibre reinforced composites in aircraft construction, Prog. Aerosp. Sci. 41 (2) (2005) 143–151.
[2] M.K. Hagnell, M. Åkermo, A composite cost model for the aeronautical industry: methodology and case study, Compos. Part B 79 (2015) 254–261.
[3] J. Studer, C. Dransfeld, K. Masania, An analytical model for B-stage joining and co-curing of carbon fibre epoxy composites, Compos. A: Appl. Sci. Manuf. 87 (2016) 282–289.
[4] A. Fink, P.P. Camanho, J.M. Andras, E. Pfeiffer, A. Obst, Hybrid CFRP/titanium bolted joints: performance assessment and application to a spacecraft payload adaptor, Compos. Sci. Technol. 70 (2) (2009) 305–317.
[5] B. Kolesnikov, L. Herbeck, A. Fink, CFRP/titanium hybrid material for improving composite bolted joints, Compos. Struct. 83 (4) (2008) 368–380.
[6] J. Studer, A. Keller, F. Leone, D. Stefaniak, C. Dransfeld, K. Masania, Local reinforcement of aerospace structures using co-curing RTM of metal foil hybrid composites, Prod. Eng. (2018) 1–7.
[7] K. Masania, R. Geissberger, F. Leone, J. Studer, D. Stefaniak, C. Dransfeld, Steel foil reinforced composites: experimental and numerical study of strength, plasticity and ply size effects, European Conf. Compos. Mater. (2014).
[8] M. Sung, J. Jang, V.L. Tran, S.-T. Hong, W.-R. Yu, Increased breaking strain of carbon fiber-reinforced plastic and steel hybrid laminate composites, Compos. Struct. 235 (2020) 111768.
[9] E. Petersen, J. Koord, O. Völkerink, D. Stefaniak, C. Hühne, Experimental and numerical investigation of the transition zone of locally steel-reinforced joining areas under combined tension–bending loading, J. Compos. Mater. 0 (0) (2019) 0021998319893729.
[10] R. Amacher, J. Cugnoni, J. Botsis, L. Sorensen, W. Smith, C. Dransfeld, Thin ply composites: experimental characterization and modeling of size-effects, Compos. Sci. Technol. 101 (2014) 121–132.
[11] C. Furtado, A. Arteiro, G. Catalanotti, J. Xavier, P. Camanho, Selective ply-level hybridisation for improved notched response of composite laminates, Compos. Struct. 145 (2016) 1–14.
[12] C. Huang, S. Ju, M. He, Q. Zheng, Y. He, J. Xiao, J. Zhang, D. Jiang, Identification of failure modes of composite thin-ply laminates containing circular hole under tension by acoustic emission signals, Compos. Struct. 206 (2018) 70–79.
[13] A. Arteiro, G. Catalanotti, J. Xavier, P. Linde, P. Camanho, A strategy to improve the structural performance of non-crimp fabric thin-ply laminates, Compos. Struct. 188 (2018) 438–449.
[14] J. Cugnoni, R. Amacher, S. Kohler, J. Brunner, E. Kramer, C. Dransfeld, W. Smith, K. Scobbie, L. Sorensen, J. Botsis, Towards aerospace grade thin-ply composites: effect of ply thickness, fibre, matrix and interlayer toughening on strength and damage tolerance, Compos. Sci. Technol. 168 (2018) 467–477.
[15] J. Galos, Thin-ply composite laminates: a review, Compos. Struct. 236 (2020) 111920.
[16] B. Bosbach, C. Ohle, B. Fiedler, Structural health monitoring of fibre metal laminates under mode I and II loading, Compos. A: Appl. Sci. Manuf. 107 (2018) 471–478.
[17] B. Kötter, J. Karsten, J. Körbelin, B. Fiedler, CFRP thin-ply fibre metal laminates: influences of ply thickness and metal layers on open hole tension and compression properties, Materials 13 (4) (2020) 910.
[18] A. Fink, P. Camanho, J. Andrés, E. Pfeiffer, A. Obst, Hybrid CFRP/titanium bolted joints: performance assessment and application to a spacecraft payload adaptor, Compos. Sci. Technol. 70 (2) (2010) 305–317.
[19] E. Petersen, J. Koord, O. Völkerink, D. Stefaniak, C. Hühne, Experimental and numerical investigation of the transition zone of locally steel-reinforced joining areas under combined tension–bending loading, J. Compos. Mater. 54 (17) (2020) 2339–2352.
[20] E. Petersen, D. Stefaniak, C. Hühne, Experimental investigation of load carrying mechanisms and failure phenomena in the transition zone of locally metal reinforced joining areas, Compos. Struct. 182 (2017) 79–90.
[21] R. Geissberger, J. Maldonado, N. Bahamonde, A. Keller, C. Dransfeld, K. Masania, Rheological modelling of thermoset composite processing, Compos. Part B 124 (2017) 182–189.

[22] K. Blohowiak, R. Anderson, W. Grace, J. Grob, D. Fry, Development of new thin adhesive systems and test methods for TiGr laminates, SAMPE conference, 2008 , Long Beach, USA.
[23] Z. Hashin, Failure criteria for unidirectional fiber composites, J. Appl. Mech. 47 (2) (1980) 329–334.
[24] G. Johnson, W. Cook, A constitutive model and data for metals subjected to large strains, strain rates, and high pressures, Proceedings of the 7th International Symposium On Ballistics, 1983.
[25] M. Ljunkrantz, Design of a CFRP-to-Steel Joint for a Bus Engine Mount and Experimental Testing of Joint Relaxation, 2012.
[26] Y. Xiao, T. Ishikawa, Bearing strength and failure behavior of bolted composite joints (part II: modeling and simulation), Compos. Sci. Technol. 65 (7–8) (2005) 1032–1043.
[27] J. Rehra, B. Hannemann, S. Schmeer, J. Hausmann, U.P. Breuer, Approach for an analytical description of the failure evolution of continuous steel and carbon fiber hybrid composites, Adv. Eng. Mater. 21 (6) (2019) 1800565.
[28] G. Czél, M. Wisnom, Demonstration of pseudo-ductility in high performance glass/epoxy composites by hybridisation with thin-ply carbon prepreg, Compos. A: Appl. Sci. Manuf. 52 (2013) 23–30.
[29] G. Czél, M. Jalalvand, M.R. Wisnom, Design and characterisation of advanced pseudo-ductile unidirectional thin-ply carbon/epoxy–glass/epoxy hybrid composites, Compos. Struct. 143 (2016) 362–370.
[30] Federal Aviation Administration, Metallic Materials Properties Development and Standardization (MMPDS), U.S. Department of Transportation, 2003.